

Article

Preparation and Application of a Fast, Naked-Eye, Highly Selective, and Highly Sensitive Fluorescent Probe of Schiff Base for Detection of Cu²⁺

Juan Liu ^{1,†}, Peng-Yu Cheng ^{1,†}, Sai Chen ¹, Meng Wang ¹, Kai Wei ¹, Yuan Li ¹, Yao-Yao Cao ¹, Xing Wang ² and Hong-Lei Li ^{1,*} 

¹ Department of Pharmacy, Kangda College of Nanjing Medical University, Lianyungang 222000, China; liujuan281@njmu.edu.cn (J.L.); cpy133386155072022@163.com (P.-Y.C.); chensai45@njmu.edu.cn (S.C.); wangmeng@njmu.edu.cn (M.W.); weikai@njmu.edu.cn (K.W.); ly15052873180@163.com (Y.L.); cyy5372649@163.com (Y.-Y.C.)

² School of Pharmacy, China Pharmaceutical University, Nanjing 211198, China; 1020132341@cpu.edu.cn

* Correspondence: lihonglei@njmu.edu.cn

[†] These authors contributed equally to this work.

Abstract: A fluorescent probe, *N'*-((3-methyl-5-oxo-1-phenyl-4, 5-dihydro-1H-pyrazol-4-yl) methylene)-2-oxo-2*H*-chromene-3-carbohydrazide (MPMC), was synthesized and characterized. Characterizations of the synthetic MPMC were conducted via proton nuclear magnetic resonance (¹H NMR) spectroscopy and carbon-13 nuclear magnetic resonance spectroscopy (¹³C NMR). The fluorescence emission behaviors of the MPMC probe towards diverse metal ions were detected, and the probe exhibited high sensitivity and selectivity towards Cu²⁺ over other metal ions via the quenching of its fluorescence. Furthermore, the existence of other metal actions made no apparent difference to the fluorescence intensity of the MPMC-Cu²⁺ system; that is, MPMC displayed a good anti-interference ability. Job's plot of the MPMC and copper ions indicated that the detection limit was 10.23 nM ($R^2 = 0.9612$) for the assayed actions, with a stoichiometric ratio of 1:1 for MPMC and Cu²⁺. Additionally, the color of the MPMC probe solution changed from nearly colorless to yellow in the presence of Cu²⁺ in visible light, and the color change could be observed by the naked eye. Similarly, the color resolved from bright yellow into blue in ultraviolet light. Moreover, reusability studies indicated that the MPMC probe was reusable. The pH effect of the MPMC probe on Cu²⁺ had a broad range of pH detection, i.e., from 4.0 to 11.0. The response time of the MPMC probe for determining Cu²⁺ was within 1 min. The recognition of Cu²⁺ via MPMC performed on pre-treated paper under sunlight and UV light both had a distinct colour change. Thus, the solid-state method for detecting Cu²⁺ with the naked eye was both economical and convenient.

Keywords: fluorescent probe of Schiff base; copper ion; high sensitivity and selectivity; good anti-interference ability; low detection limit



Citation: Liu, J.; Cheng, P.-Y.; Chen, S.; Wang, M.; Wei, K.; Li, Y.; Cao, Y.-Y.; Wang, X.; Li, H.-L. Preparation and Application of a Fast, Naked-Eye, Highly Selective, and Highly Sensitive Fluorescent Probe of Schiff Base for Detection of Cu²⁺. *Chemosensors* **2023**, *11*, 556. <https://doi.org/10.3390/chemosensors11110556>

Academic Editors: Ambra Giannetti and Young-Tae Chang

Received: 7 October 2023

Revised: 31 October 2023

Accepted: 2 November 2023

Published: 6 November 2023



Copyright: © 2023 by the authors. Licensee MDPI, Basel, Switzerland. This article is an open access article distributed under the terms and conditions of the Creative Commons Attribution (CC BY) license (<https://creativecommons.org/licenses/by/4.0/>).

1. Introduction

Copper (II) ion is one of the essential transition metal ions that play a crucial role in many key physiological processes in living organisms, including electron transport oxidoreductases, the production of hemocyanin, blue copper protein, cytochrome C oxidase, lactase, ascorbate oxidase, superoxide dismutase, skin pigmentation, and connective tissue repair [1–3]. However, excessive amounts of Cu²⁺ can lead to a variety of diseases, such as induction of cell death, Parkinson's, Alzheimer's, and prion diseases [4–6]. In addition, the widespread use of Cu²⁺ in the electronic and electrical industries makes it an environmental pollutant. Especially in recent years, the operations of ore mining along with metals extraction in nature are growing, which brings about severe heavy metals pollution (copper, cadmium, etc.) in the atmosphere, water resources, and soil. These heavy metals are

incapable of being degraded by organisms; instead, they can be enriched thousands of times via the biomagnification of food chain; then, they intrude into the human body, making them a serious health hazard [7,8]. Consequently, the development of a highly sensitive and selective Cu^{2+} assay for the efficient detection of Cu^{2+} in aqueous solutions or biological systems is of great importance for biology, clinical medicine, chemistry, and environmental sciences.

Nowadays, various detection technologies have been developed to test Cu^{2+} , such as chemiluminescence [9], electro-chemistry [10], colorimetry [11], atomic absorption spectrometry [12], and inductively coupled plasma mass spectrometry [13]. However, these detection strategies have the drawbacks of low sensitivity and cumbersome operation. In recent years, fluorescent molecular probes have been rapidly developing in molecular recognition because of their excellent recognition properties, high selectivity, and sensitivity, being accessible in site detection and real-time imaging. The “host–guest” pattern is a fundamental structural model of fluorescent probes, including, chiefly, fluorophore and receptor, connected by covalent bonding through a spacer. Recognition units that possess different recognition functions serve to grasp and recognize test samples. Meanwhile, for the difference of molecular structure before and after grasping, fluorophore’s fluorescence property displays different fluorescence signals (wavelength or intensity variation), so as to achieve the purpose of recognition and detection [14–17]. Actually, most fluorescent probes that identify Cu^{2+} are restricted in their applications for the poor selectivity, short wavelength emission, interference from autofluorescence, the need for a high organic phase detection environment, and the presence of many possible interfering agents.

Coumarin (2*H*-1-benzopyran-2-one), a fluorophore used extensively, possesses high fluorescence quantum yields, good photostability, large Stokes shifts, and easy structural modifications. Coumarin derivatives have been found in various plants, which are widely used in aqueous environmental monitoring, antibacterial and antitumor medications, and others [18]. Currently, coumarin-based fluorescent probes consist essentially of Schiff bases [19–22] and biological thiols [23,24]. In particular, a few studies on the coumarin-based pyrazolone fluorescent probes have been reported [23–25].

In the field of analytical chemistry, as a conjugated double bond, Schiff bases are recommended for the detection and identification of metal ions. Additionally, Schiff bases are applied to the quantitative analysis of certain ions by means of chromatography, fluorescence analysis, and photometric analysis. Meanwhile, for the space-turning effect of $-\text{C}=\text{N}-$ in the molecular structure, Schiff bases and their complexes tend to coordinate easily. In addition, lone-pair electrons of the integral structure are more abundant, such that the coordination sites also become more abundant, which indicates that Schiff bases have good, coordinated properties. At this stage, Schiff bases make coordination with metallic cations easier, especially the heavy metal ions. Thus, Schiff bases are good ligands for metal ions [19–22].

Thus, a fluorescent probe based on coumarin and pyrazole Schiff base, *N'*-((3-methyl-5-oxo-1-phenyl-4, 5-dihydro-1*H*-pyrazol-4-yl) methylene)-2-oxo-2*H*-chromene-3-carbohydrazide (MPMC), was designed and synthesized in this paper [26]. The coumarin moiety belonging to MPMC served as the fluorophore; and the acylhydrazone structure belonging to MPMC served as the recognition receptor and bursting part. The results demonstrate that the MPMC probe was selective and sensitive for the detection of Cu^{2+} .

2. Experiments

2.1. Reagents and Chemicals

Phenylhydrazine (molecular weight: 108.14; relative density: 1.099 g/mL at 25 °C; and CAS number: 100-63-0), and 2-hydroxybenzaldehyde (molecular weight: 122.12; relative density: 1.146 g/mL at 25 °C; and CAS number: 90-02-8) were both analytical reagents, purchased from Macklin Inc. (Shanghai, China). Piperidine (molecular weight: 85.15; relative density: 0.862 g/mL at 20 °C; and CAS number: 110-89-4) was of analytical grade and purchased from TCI chemicals (Shanghai, China). Ethyl acetoacetate (molecular

weight: 130.14; relative density: 1.029 g/mL at 20 °C; and CAS number: 141-97-9), an analytical reagent, was obtained from Aladdin Inc. (Shanghai, China). A total of 85% hydrazine hydrate (molecular weight: 50.06; relative density: 1.03 g/mL at 25 °C; and CAS number: 7803-57-8), was of analytical grade and obtained from Nanjing Reagent (Nanjing, China). Phosphoric trichloride (molecular weight: 153.33; relative density: 1.645 g/mL at 25 °C; and CAS number: 10025-87-3), analytical grade, was purchased from Kaiwei Chemical (Shanghai, China). Diethyl malonate (molecular weight: 160.17; relative density: 1.055 g/mL at 25 °C; and CAS number: 105-53-3), anhydrous ethanol (molecular weight: 46.07, relative density: 0.789 g/mL at 20 °C; and CAS number: 64-17-5), 36% acetic acid (molecular weight: 60.05; relative density: 1.05 g/mL at 25 °C; and CAS number: 64-19-7), hydrochloric acid (molecular weight: 36.46; relative density: 1.17 g/mL at 20 °C; and CAS number: 7647-01-0), *N,N*-dimethylformamide (molecular weight: 73.09; relative density: 0.948 g/mL at 20 °C; and CAS number: 68-12-2), sodium hydroxide (molecular weight: 40.01; relative density: 2.12 g/mL at 20 °C; and CAS number: 1310-73-2), cupric chloride anhydrous (molecular weight: 134.45; relative density: 3.386 g/mL at 25 °C; and CAS number: 7447-39-4), zinc chloride (molecular weight: 136.30; relative density: 1.01 g/mL at 20 °C; and CAS number: 7646-85-7), manganese(II) chloride (molecular weight: 125.84; relative density: 2.98 g/mL at 25 °C; and CAS number: 7773-01-5), nickel(II) sulfate (molecular weight: 154.76; relative density: 3.68 g/mL at 25 °C; and CAS number: 7786-81-4), iron(III) chloride (molecular weight: 162.20; relative density: 2.84 g/mL at 25 °C; and CAS number: 7705-08-0), ferrous chloride (molecular weight: 126.75; relative density: 3.16 g/mL at 25 °C; and CAS number: 7758-94-3), calcium chloride (molecular weight: 110.98; relative density: 1.086 g/mL at 25 °C; and CAS number: 10043-52-4), magnesium sulfate (molecular weight: 120.37; relative density: 1.07 g/mL at 25 °C; and CAS number: 7487-88-9), lead chloride (molecular weight: 278.11; relative density: 5.85 g/mL at 25 °C; and CAS number: 7758-95-4), sodium chloride (molecular weight: 58.44; relative density: 2.165 g/mL at 25 °C; and CAS number: 7647-14-5), potassium chloride (molecular weight: 74.55; relative density: 1.98 g/mL at 25 °C; and CAS number: 7447-40-7), silver nitrate (molecular weight: 169.87; relative density: 4.35 g/mL at 25 °C; and CAS number: 7761-88-8), and barium chloride (molecular weight: 208.23; relative density: 3.856 g/mL at 25 °C; and CAS number: 10361-37-2) were all of analytical grade, and obtained from Sinopharm (Shanghai, China). A stock solution of MPMC was prepared in EtOH at a concentration of 1.0×10^{-3} mol/L. The stock perchlorate solutions (including the perchlorate of Cu^{2+} , Pb^{2+} , Fe^{3+} , Fe^{2+} , Mg^{2+} , Ni^{2+} , Cd^{2+} , Co^{2+} , Mn^{2+} , Ca^{2+} , Ba^{2+} , Na^{+} , K^{+} , Zn^{2+} and Ag^{+}) were freshly prepared in deionized water at a concentration of 1.0×10^{-3} mol/L.

^1H and ^{13}C NMR spectra were recorded on a Bruker AVANCE III 400 MHz NMR spectrometer in $\text{DMSO-}d_6$ with TMS as an internal standard. Mass spectrum was recorded on the Thermo Q-Exact mass spectrometer. The melting point was measured on the XRC-1 melting point instrument. The ultraviolet absorption was recorded on Cary50. The fluorescence test was recorded on the RF-6000 luminescence spectrophotometer. ESI-MS data were recorded with Mariner System 5304 mass spectrometer. Elemental analyses (C, H, and N) were gathered on a CHN-O-Rapid instrument within 0.4% of the theoretical values.

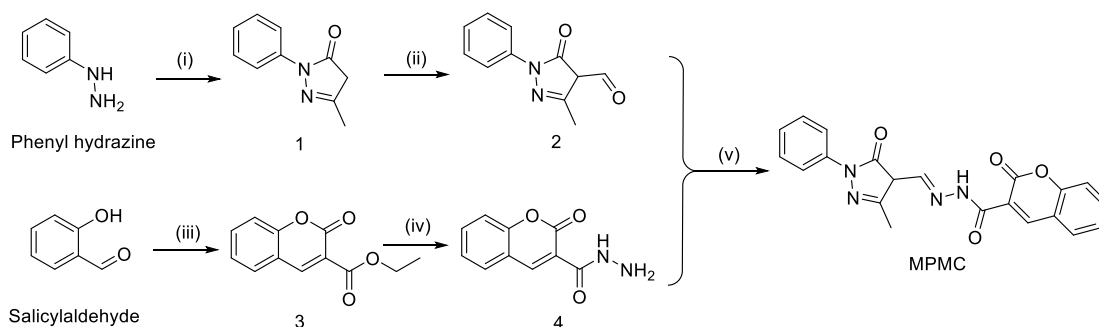
2.2. Synthesis of MPMC

The synthetic route of the target MPMC probe is shown in Scheme 1. Edaravone aldehyde derivative (compound 2) and coumarin-3-carbohydrazide (compound 4) were synthesized in reference to the methods reported in the literature [27–30].

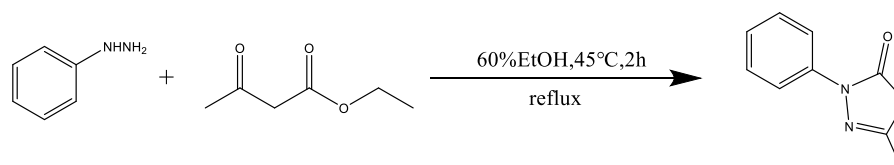
2.2.1. Synthesis of Edaravone

A total of 13.0 g and 0.1 mol of acetyl ethyl acetate was first mixed with 5 mL of 60% ethanol solution while stirring. Next, a solution consisting of phenylhydrazine (10.8 g, 0.1 mol) and absolute ethanol was added dropwise at 45 °C in approximately 30 min. After dripping, the reaction proceeded at 45 °C for 20 min. Thereafter, the reaction solution was cooled to room temperature, supplemented with 1 mL of concentrated hydrochloric acid,

reacting at 45 °C for another 2 h. The following is the addition of 10% sodium hydroxide solution, dropwise, to adjust the pH to be 7.0. Then, the solution was added by 20 mL of water and stirred at room temperature for 1 h, followed by filtering to obtain light yellow crystals. Finally, crystals were washed with cold absolute ethanol and heated to reflux in ethyl acetate and absolute ethanol solution (with a volume ratio of 2:1) to obtain white and pure edaravone (compound 1). The synthetic route of edaravone is shown in Scheme 2.



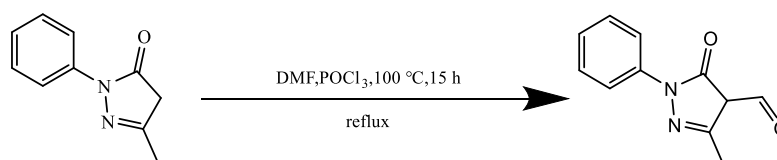
Scheme 1. Reagents and conditions: (i) ethyl acetoacetate, 60% ethanol solution, 45 °C, 2 h; (ii) N,N-dimethylformamide, POCl₃, 100 °C, 15 h; (iii) diethyl malonate, piperidine, ethanol, 25 °C, overnight; (iv) ethanol, 85% hydrazine hydrate, 20 h; (v) ethanol, CH₃COOH, reflux, 2 h.



Scheme 2. Synthesis of edaravone.

2.2.2. Synthesis of Edaravone Aldehyde Derivative

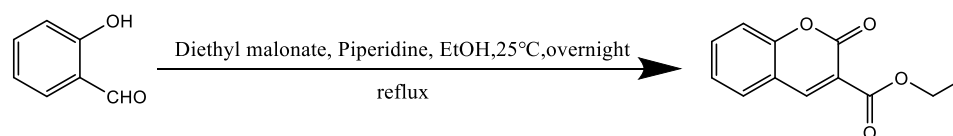
Edaravone (8.70 g, 0.05 mol) was dissolved in 1 mL of N,N-dimethylformamide under stirring; then, 10.1 mL of phosphorus oxychloride was introduced slowly in drops by an external ice bath. The reaction mixture was then heated to reflux for 1.5 h. After cooling, it was introduced into 200 mL of ice water, then oscillated, stood still, and filtered; thus, crude edaravone aldehyde derivative was obtained. Subsequently, the crude product was treated by absolute ethanol washing, heated to reflux in ethanol, followed by drying to gain the pure edaravone aldehyde derivative (compound 2). The synthetic route of edaravone aldehyde derivative is shown in Scheme 3.



Scheme 3. Synthesis of edaravone aldehyde derivative.

2.2.3. Synthesis of Ethyl Coumarin-3-Carboxylate

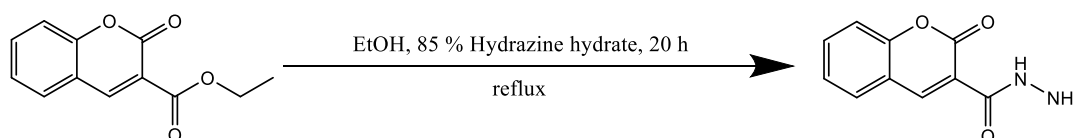
Salicylaldehyde (4.90 g, 0.04 mol), diethyl malonate (7.25 g, 0.045 mol), and 20 mL of absolute ethanol were successively added and thoroughly mixed, and then 0.5 mL of hexahydropyridine and two drops of acetic acid were dripped. In succession, the reaction mixture was then heated to reflux for 2 h while stirring. After being cooled to dilution crystallization, filtering was adopted to obtain the crude product, which was then washed with ethanol several times and dried to obtain the pure ethyl coumarin-3-carboxylate (compound 3). The synthetic route of ethyl coumarin-3-carboxylate is shown in Scheme 4.



Scheme 4. Synthesis of ethyl coumarin-3-carboxylate.

2.2.4. Synthesis of Coumarin-3-Carbohydrazide

In the presence of coumarin-3-carboxylic acid ethyl ester (2.00 g, 0.01 mol) and 50 mL of anhydrous ethanol, five drops of hydrazine hydrate (0.01 mol) were then added. The reaction mixture was heated to reflux for 10 h under agitation. Then, crystals of coumarin-3-carbohydrazide were formed while being cold. After filtering, yellow crystals were obtained. The yellow crystals were washed by absolute ethanol and dissolved with reflux in absolute ethanol. Finally, bright yellow crystals, which were the pure coumarin-3-carbohydrazide (compound 4), were produced via the dryness. The synthetic route of coumarin-3-carbohydrazide is shown in Scheme 5.



Scheme 5. Synthesis of coumarin-3-carbohydrazide.

2.2.5. Synthesis of MPMC Probe

Compound 2 (1.0 g, 4.95 mmol) and compound 4 (1.0 g, 4.95 mmol) were dissolved in 40 mL of ethanol. With the addition of catalyst acetic acid, the reaction proceeded at reacting temperature of 78 °C, heating to reflux for 2 h. After restoration at room temperature, a light-yellow precipitate was generated and was obtained via filtering, washing with ethanol several times. Finally, the precipitate was dried to give the MPMC probe (0.902 g, yield 46.96%). m.p. > 280 °C. ¹H NMR and ¹³C NMR data of MPMC are shown as follows: ¹H NMR (400 MHz, DMSO-*d*₆) δ 11.14 (s, 1H), 9.01 (s, 1H), 8.77 (s, 1H), 7.93 (d, *J* = 7.6 Hz, 1H), 7.76 (d, *J* = 8.0 Hz, 1H), 7.73–7.68 (m, 1H), 7.45 (d, *J* = 8.6 Hz, 1H), 7.44–7.37 (m, 2H), 7.00 (s, 1H), 6.97 (d, *J* = 7.4 Hz, 1H), 4.30 (q, *J* = 7.0 Hz, 2H), 1.32 (t, *J* = 7.1 Hz, 3H). ¹³C NMR (100 MHz, DMSO-*d*₆) δ 163.26, 163.07, 159.11, 156.48, 155.01, 149.19, 134.97, 133.72, 131.28, 130.76, 125.33, 120.08, 118.66, 118.29, 118.14, 117.00, 116.63, 61.71, 14.54. MS (ESI): 389.38 (M + H)⁺. Anal. Calcd for C₂₁H₁₆N₄O₄: C, 64.94; H, 4.15; N, 14.43. Found: C, 64.92; H, 4.13; N, 14.41.

2.3. General Procedure for the Spectrum Measurement

Stock solutions of MPMC (1 mM) were prepared in ethanol. The metal ions stock solutions (1 mM) were prepared with the nitrate or chloride salts (Cu²⁺, Pb²⁺, Fe³⁺, Fe²⁺, Mg²⁺, Ni²⁺, Cd²⁺, Co²⁺, Mn²⁺, Ca²⁺, Ba²⁺, Na⁺, K⁺, Zn²⁺ and Ag⁺) in deionized water. Absorption and emission spectra were obtained at room temperature using PBS solution (pH 7.5) in MPMC (10 μM) with different concentrations of analyzer. Fluorescence spectra were recorded at an excitation wavelength of 358 nm. The total concentration of Cu²⁺ and MPMC was kept constantly (2.0 mM). The fluorescence intensity of MPMC was then recorded by varying the molar ratio of MPMC to Cu²⁺. The selectivity of MPMC towards Cu²⁺ was tested by comparing other metal ions. MPMC (1 mM) was treated with Cu²⁺ (1 mM) and other metal ions (10 mM) for 10 min and the fluorescence intensity of the mixtures was recorded. For reproducibility testing, Cu²⁺ (1.0 mM) was incubated with MPMC aqueous solution (1.0 mM), and the fluorescence of MPMC was quenched. The fluorescence intensity of MPMC (1.0 mM) and MPMC-Cu²⁺ ensemble (1.0 mM) was determined in a series of buffers (pH 1.0 to 14.0).

3. Results and Discussion

3.1. Fluorescence Spectra of the MPMC Probe for Selectivity and Anti-Interference Detection

The fluorescence emission behaviors of the MPMC probe towards diverse metal ions were detected in ethanol (EtOH)/H₂O (*v/v* = 1/1) solution, respectively. Fluorescence intensities of diverse metal ions added to MPMC were detected as the wavelength variation. The fluorescence emission spectrums are illustrated in Figure 1a. As shown in Figure 1a, when excitation wavelength 358 nm was given to the MPMC probe, a fluorescence emission band at 548 nm generated. Then fluorescence quenching followed along with the insertion of Cu²⁺ (1.0 equiv), with the emission minimum being at 548 nm. Conversely, the fluorescence emission spectrums of MPMC were affected little by introducing other metal ions, in addition to a weak quenching of nickel ions.

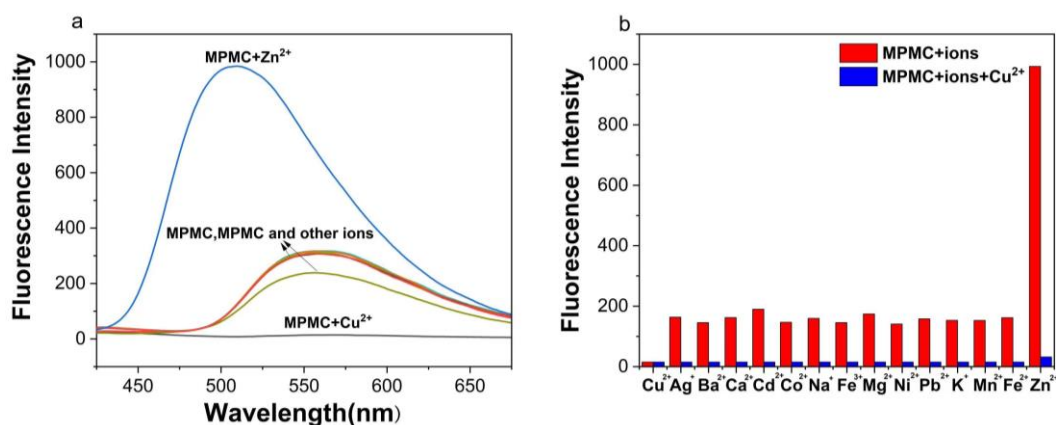


Figure 1. (a) Fluorescence emission spectra of the MPMC probe (10 μM) without or with metal ions (including Cu²⁺, Pb²⁺, Fe³⁺, Fe²⁺, Mg²⁺, Ni²⁺, Cd²⁺, Co²⁺, Mn²⁺, Ca²⁺, Ba²⁺, Na⁺, K⁺, Zn²⁺, Ag⁺) (10 μM) in ethanol with excitation wave length of 358 nm. (b) Fluorescence response of MPMC (10 μM) to Cu²⁺ in the presence of various metal ions (including Pb²⁺, Fe³⁺, Fe²⁺, Mg²⁺, Ni²⁺, Cd²⁺, Co²⁺, Mn²⁺, Ca²⁺, Ba²⁺, Na⁺, K⁺, Zn²⁺, Ag⁺) (100 μM) in EtOH/H₂O (*v/v* = 1/1) (λ_{ex} = 358 nm, λ_{em} = 548 nm).

Furthermore, in view of potential interference of other metal ions in practical applications, sorts of metal ions were added successively into the MPMC-Cu²⁺ system, and the influences on fluorescence selectivity were investigated.

A total of 100 μM of competitive metal ions (Pb²⁺, Fe³⁺, Fe²⁺, Mg²⁺, Ni²⁺, Cd²⁺, Co²⁺, Mn²⁺, Ca²⁺, Ba²⁺, Na⁺, K⁺, Zn²⁺, Ag⁺), along with 10 μM MPMC in EtOH-H₂O (*v/v* = 1/1), were prepared and determined to access the fluorescence intensities. As Figure 1b illustrates, a fluorescence emission band at 548 nm was generated again. Thereafter, with the addition of 10 μM Cu²⁺, the fluorescence quenching took place. The existence of other metal actions made no difference on the fluorescence intensity apparently. In general, the MPMC probe has the characteristic of selectively recognizing Cu²⁺, displaying a good anti-interference ability.

3.2. Titration Experiment of the MPMC Probe to Cu²⁺

Colorimetric experiments were conducted to study the specificity of the MPMC probe towards Cu²⁺. As Figure 2a shows, while adding Cu²⁺ to MPMC dissolved in EtOH/H₂O (*v/v* = 1/1), the color of solution passed from colorless to yellow in seconds. The result shows that the MPMC probe can realize the colorimetric detection of Cu²⁺ with a detection limit 10 μM . In the same way, the fluorescence color turned from colorless to yellow under 365 nm ultraviolet (UV) light, shown in Figure 2b. The applied results clearly demonstrate that the MPMC probe could have an application in the qualitative and quantitative detection of Cu²⁺ in the form of color change and spectrum signals multiplication.

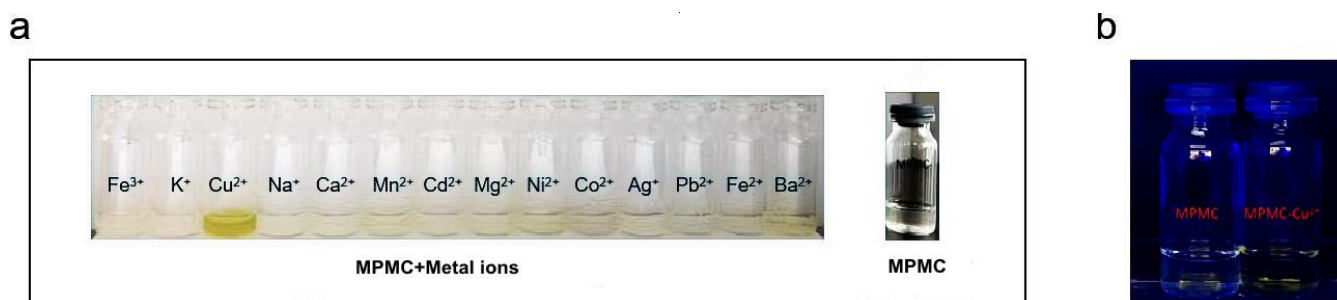


Figure 2. (a) Colorimetric performance of sensor MPMC (1 mM) upon addition of different metal ions (including Cu^{2+} , Pb^{2+} , Fe^{3+} , Fe^{2+} , Mg^{2+} , Ni^{2+} , Cd^{2+} , Co^{2+} , Mn^{2+} , Ca^{2+} , Ba^{2+} , Na^+ , K^+ , Ag^+) (1 mM) in EtOH/ H_2O ($v/v = 1/1$) solution; (b) color change induced upon addition of Cu^{2+} under 365 nm UV lamp.

As the concentration variation of Cu^{2+} , fluorescence titration experiments were performed to explore the sensitivity of the MPMC probe to Cu^{2+} . As illustrated in Figure 3, with the Cu^{2+} concentration rising, the fluorescence intensity of the MPMC probe reflected a continued decrease. The linear equation for copper (II) ions is $Y = -728.21X + 1388.2$, and the correlated coefficient is 0.9612. Based on the formula $L = 3\sigma/Ka$, the minimum detectable concentration of the probe for copper (II) ions was calculated as 10.23 nM [31]. Compared with other fluorescent probes for the detection of Cu^{2+} listed in Table 1, the MPMC probe prepared in this paper has a lower detection limit.

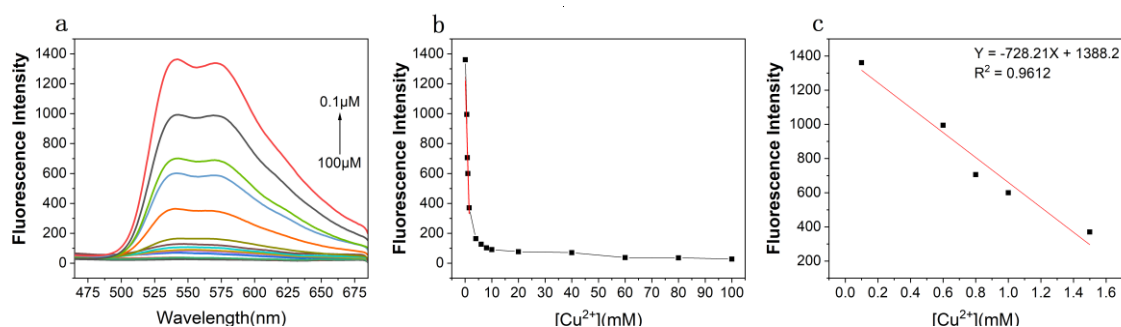


Figure 3. (a) The fluorescence spectra of MPMC (10 μM) with the increasing concentration of Cu^{2+} ion (0.01–10.0 equiv.) in EtOH/ H_2O ($v/v = 1/1$). (b) The changes of fluorescence signal with different concentrations of copper ions. (c) The linear fit between MPMC and Cu^{2+} .

Table 1. Performance of MPMC compared with available Cu^{2+} probes.

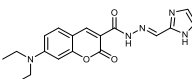
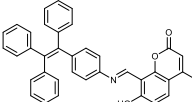
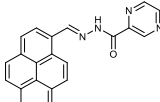
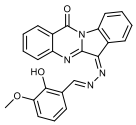
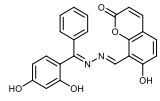
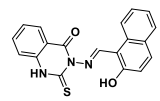
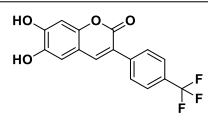
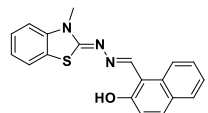
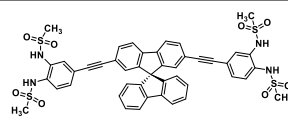
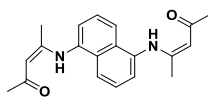
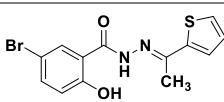
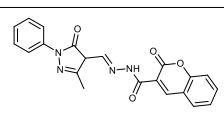
Compound	Molecular Formula	Solvent	Repeatability	Detection Limit	Reference
	$\text{C}_{18}\text{H}_{19}\text{N}_5\text{O}_3$	$\text{CH}_3\text{CN}:\text{HEPES}$ (3:2, v/v)	No	0.12 μM	[20]
	$\text{C}_{37}\text{H}_{27}\text{NO}_3$	THF/ H_2O	No	0.36 μM	[22]
	$\text{C}_{22}\text{H}_{14}\text{N}_4\text{O}$	EtOH-HEPES	No	157 nM	[32]

Table 1. Cont.

Compound	Molecular Formula	Solvent	Repeatability	Detection Limit	Reference
	C ₂₃ H ₁₆ N ₄ O ₃	Tris-HCl buffer solution	Yes	84 nM	[33]
	C ₂₃ H ₁₆ N ₂ O ₅	EtOH-HEPES (80:20, v/v)	No	6.14 × 10 ⁻⁷ M	[34]
	C ₁₉ H ₁₃ N ₃ O ₂ S	DMSO:H ₂ O (1:9, v/v)	No	20.0 nM	[35]
	C ₁₆ H ₉ F ₃ O ₄	CH ₃ CN/HEPES (95/5, v/v)	No	24.5 nM	[36]
	C ₁₉ H ₁₅ N ₃ O ₃ S	DMSO	No	3.3 μM	[37]
	C ₄₅ H ₃₆ N ₄ O ₈ S ₄	50% CH ₃ CN and 20 mM HEPES	No	390 nM	[38]
	C ₂₀ H ₂₂ N ₂ O ₂	Water/DMF (9.9/0.1)	No	-	[39]
	C ₁₃ H ₁₁ BrN ₂ O ₂ S	DMSO	No	2.35 μM	[40]
	C ₂₁ H ₁₆ N ₄ O ₄	EtOH/H ₂ O (1:1, v/v)	Yes	10.23 nM	This work

3.3. Study of EDTA Effect of MPMC Probe on Cu²⁺

To fully investigate the response between MPMC probe and Cu²⁺, the procedures involved the addition of ethylene diamine tetraacetate acid (EDTA) to MPMC-Cu²⁺ complex, and the detection of fluorescence intensity was performed. As shown in Figure 4, the fluorescence intensity was recovered with the additional amount of EDTA added into the MPMC-Cu²⁺ complex. It suggests that the complexation ability of EDTA to Cu²⁺ is stronger than that of the MPMC probe. EDTA seized the Cu²⁺ bound to the MPMC probe, leading to the recovery of fluorescence. Namely, the fluorescence recognition between MPMC probe and Cu²⁺ is reversible [41]. Then, the fluorescence quenching still occurred after the sustainable addition of Cu²⁺. Similarly, the fluorescence intensity recovered again after the addition of EDTA. The results indicate that the MPMC probe is reusable.

3.4. Study of pH Effect of MPMC Probe to Cu²⁺

The MPMC probe is required not only for highly sensitive and selective performance, but also for its good sensing ability at different acidities in practical applications. The sensing ability was detected by adjusting the pH of EtOH-PBS (phosphate buffer solution) from

1.0 to 14.0. As Figure 5 illustrates, with a range 4.0–11.0 of pH variation, the fluorescence intensity of the MPMC probe was maintained constantly. It then dropped dramatically in a range 5.0–8.0 pH while adding Cu^{2+} to the MPMC solution. At a low pH range, the fluorescence intensity exhibited no variance; it was probably caused by hydrolysis of Cu^{2+} under acidic conditions, which inhibited the formation of the MPMC- Cu^{2+} complex³⁰. Thus, the prepared MPMC probe acted as a fluorescent pH sensor, suitable for a broad range of pH detection (4.0 to 11.0), especially from 5.0 to 8.0.

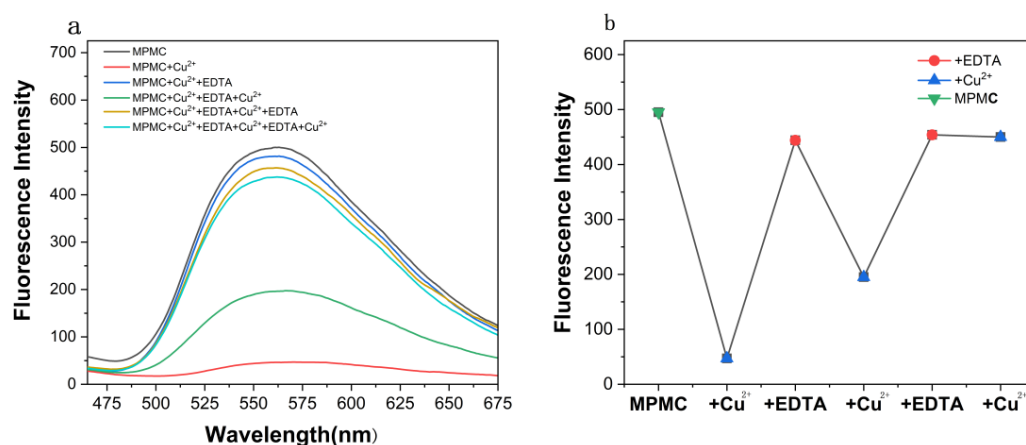


Figure 4. (a) The fluorescence spectra of MPMC in the presence of Cu^{2+} and EDTA in EtOH/ H_2O ($v/v = 1/1$) ($\lambda_{\text{ex}} = 358 \text{ nm}$, $\lambda_{\text{em}} = 548 \text{ nm}$). (b) Changes in emission spectra of MPMC in the presence of Cu^{2+} and EDTA in EtOH/ H_2O ($v/v = 1/1$) ($\lambda_{\text{ex}} = 358 \text{ nm}$, $\lambda_{\text{em}} = 548 \text{ nm}$).

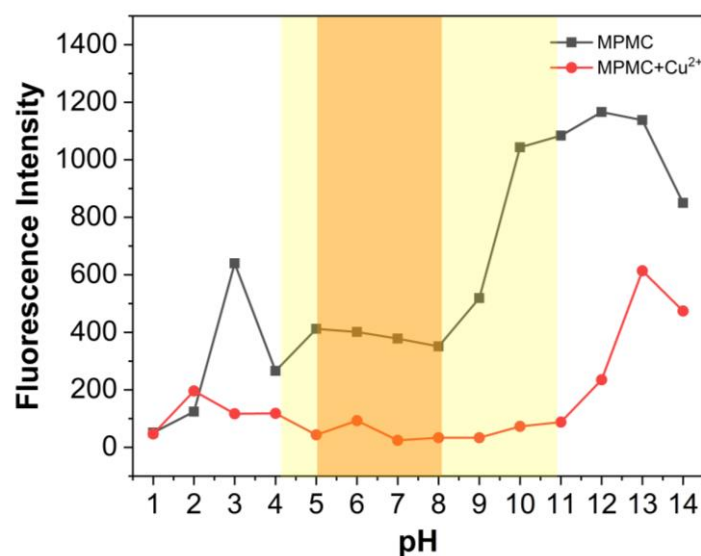


Figure 5. Fluorescence intensity changes of MPMC probe (black line) and MPMC- Cu^{2+} complexes (red line) under different pH values in phosphate buffer system ($\lambda_{\text{ex}} = 358 \text{ nm}$, $\lambda_{\text{em}} = 548 \text{ nm}$).

3.5. Study of the Response Time of MPMC Probe to Cu^{2+}

The response time of the MPMC probe in determining copper (II) ions was obtained. The variation of the fluorescence intensity at 548 nm with the reaction time of the MPMC probe along with Cu^{2+} is shown in Figure 6. After the addition of copper (II) ions, the fluorescence intensity of the MPMC probe declined markedly within 1 min then achieved an equilibrium after 2 min.

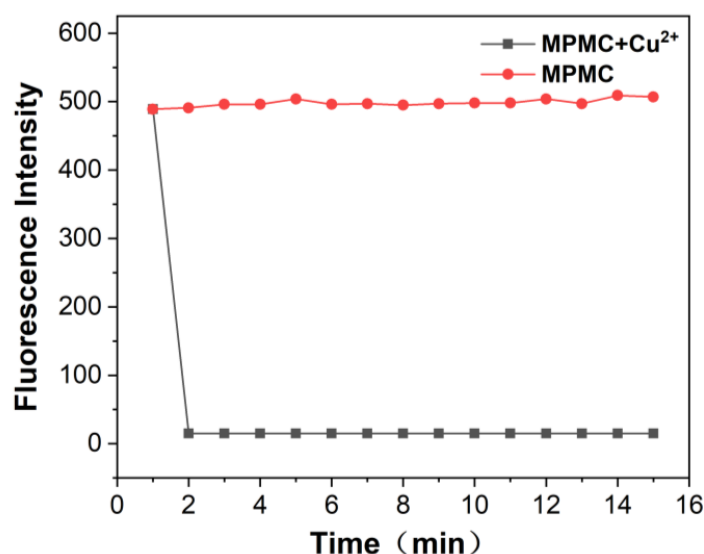


Figure 6. Time-dependent changes of MPMC (10 μM) (black line) with the addition of Cu^{2+} (10 μM) (red line) in EtOH/ H_2O ($v/v = 1/1$) ($\lambda_{\text{ex}} = 358 \text{ nm}$, $\lambda_{\text{em}} = 548 \text{ nm}$).

3.6. Contact Mode Detection between MPMC Probe and Cu^{2+}

To explore the binding ratio of the MPMC probe to Cu^{2+} , different ratios of the MPMC probe to Cu^{2+} (1:9, 2:8, 3:7, 4:6, 5:5, 6:4, 7:3, 8:2, 9:1) were prepared. As the molar fraction changed, the fluorescence characteristics were analyzed, and Job's plot curve is illustrated in Figure 7. With the molar fraction varying from 1:9 to 5:5, the fluorescence intensity decreased first, while the fluorescence intensity was almost unchanged in the range from 5:5 to 9:1. The molar fraction corresponding to the minimum fluorescence intensity of the MPMC probe appeared at 0.5, indicating that MPMC- Cu^{2+} complex was formed by 1:1. The possible binding mechanism of MPMC to Cu^{2+} -induced fluorescence changes is shown in Figure 8.

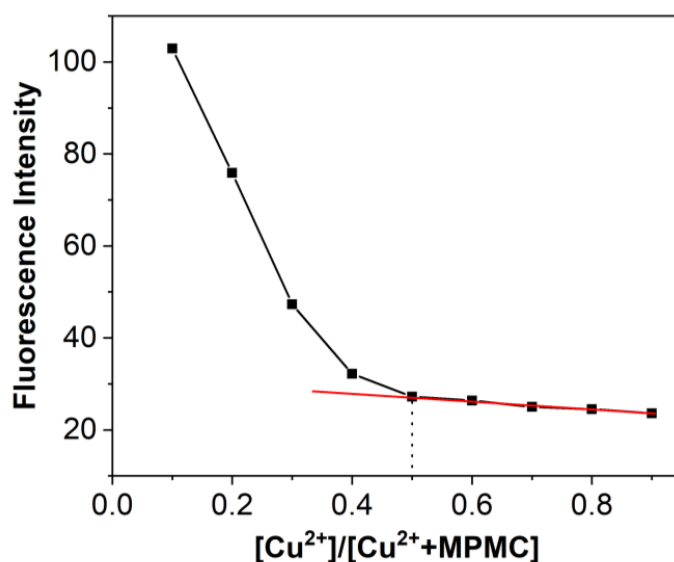


Figure 7. Job's plot of MPMC and copper ions ($[\text{MPMC}] + [\text{Cu}^{2+}] = 20 \mu\text{M}$) in EtOH/ H_2O ($v/v = 1/1$) by fluorescence spectra, where the fluorescence intensity at 548 nm was plotted against the mole fraction of $[\text{Cu}^{2+}]/([\text{MPMC}] + [\text{Cu}^{2+}])$.

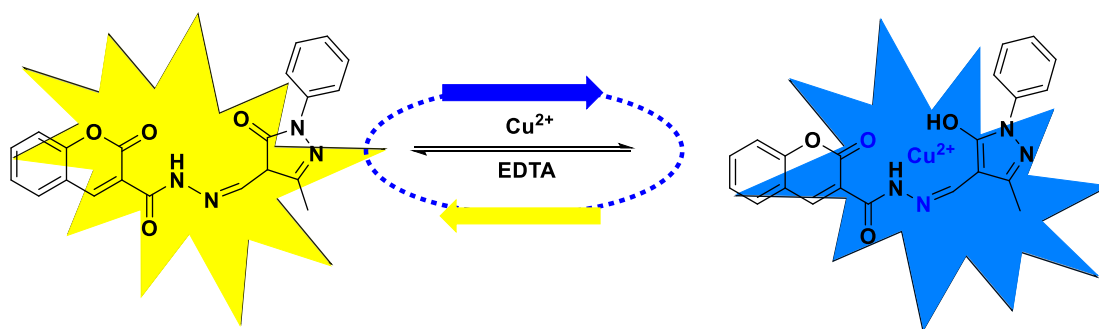


Figure 8. The proposed sensing mechanism of MPMC to Cu^{2+} in the system.

3.7. The Test Paper for Cu^{2+} Ions

To study the multifunction applications of the solid-state MPMC probe for its high efficiency and simplicity, the recognition of Cu^{2+} by MPMC was performed on pre-treated paper. Filter papers were steeped in MPMC probe dissolved in an ethanol-saturated solution (1.0×10^{-3} mol/L) for a few seconds to obtain test strips. Afterward, solid-state experiments were carried out by drying test strips in air and treating with an aqueous solution of Cu^{2+} (1.0×10^{-3} mol/L). Under sunlight, test strips before and after solid-state experiments presented white and yellow colors, respectively, as seen in Figure 9. In the same way, the color became light yellow and blue under 365 nm UV light, respectively [42]. Thus, the solid-state method for detecting Cu^{2+} with the naked eye was both economical and convenient.

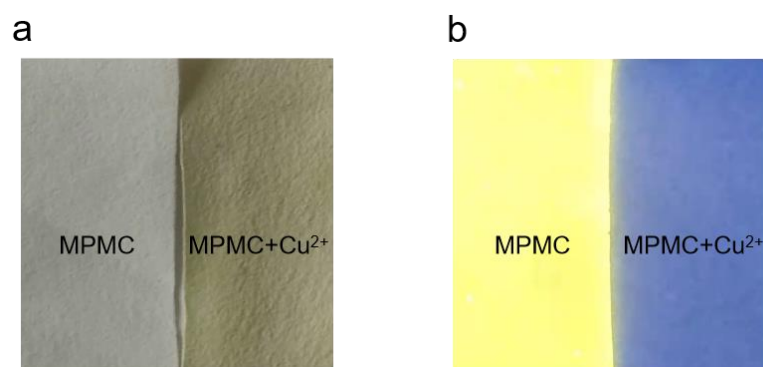


Figure 9. Photographs showing the color changes of the MPMC probe (1.0 mM) before and after addition of Cu^{2+} (1.0 mM) under (a) sunlight and (b) 365 nm UV light.

4. Conclusions

A fluorescent probe with highly selective and sensitive performance based on coumarin and pyrazole Schiff base has been synthesized. The fluorescence emission behaviors of the MPMC probe towards diverse metal ions were detected, and the probe exhibited high sensitivity and selectivity towards Cu^{2+} over other metal ions via the quenching of its fluorescence. Furthermore, the existence of other metal actions made no apparent difference to the fluorescence intensity of the MPMC- Cu^{2+} system; that is, MPMC displayed a good anti-interference ability. Job's plot of MPMC and copper ions indicated that the detection limit was 10.23 nM ($R^2 = 0.9612$) for the assayed actions, with a stoichiometric ratio of 1:1 for MPMC and Cu^{2+} . Additionally, the color of the MPMC probe solution changed from nearly colorless to yellow in the presence of Cu^{2+} in visible light, and the color change could be observed by the naked eye. Similarly, the color resolved from bright yellow into blue in ultraviolet light. Moreover, the MPMC probe was reusable. The pH effect of the MPMC probe on Cu^{2+} had a broad range of pH detection (4.0 to 11.0, especially from 5.0 to 8.0). The response time of the MPMC probe for determining Cu^{2+} was within 1 min. The recognition of Cu^{2+} by MPMC performed on pre-treated paper under sunlight and UV

light both had a distinct colour change. In conclusion, the MPMC probe could be applied to recognize Cu^{2+} in the environment; moreover, applications in biological systems may be achieved in future.

Author Contributions: Conceptualization, H.-L.L., J.L., P.-Y.C. and X.W.; Data curation, H.-L.L., J.L., P.-Y.C., X.W., M.W., K.W., Y.L. and Y.-Y.C.; Formal Analysis, P.-Y.C., S.C., M.W., K.W., Y.L. and Y.-Y.C.; Funding acquisition, H.-L.L., J.L., S.C. and M.W.; Investigation, J.L., P.-Y.C., S.C., M.W., K.W., Y.L. and Y.-Y.C.; Methodology, H.-L.L. and P.-Y.C.; Project administration, H.-L.L., J.L., P.-Y.C. and X.W.; Resources, H.-L.L., J.L. and X.W.; Supervision, H.-L.L. and X.W.; Validation, J.L., P.-Y.C., S.C., M.W., K.W., Y.L. and Y.-Y.C.; Visualization, H.-L.L., J.L., P.-Y.C., X.W., S.C., M.W., K.W., Y.L. and Y.-Y.C.; Writing—original draft, H.-L.L., J.L., P.-Y.C. and X.W.; Writing—review and editing, H.-L.L., J.L., P.-Y.C., X.W., S.C., M.W., K.W., Y.L. and Y.-Y.C. All authors have read and agreed to the published version of the manuscript.

Funding: This research was funded by the Scientific Research Personnel Training Program of Kangda College of Nanjing Medical University (No. KD2022KYRC007, Kangda College of Nanjing Medical University), the Science and Technology Funds of Nanjing Medical University (No. NMUB20210365, Nanjing Medical University), the Social Development Funds of Lianyungang (No. SF2107, Lianyungang Science and Technology Bureau), the Science and Technology Funds of Kanada College of Nanjing Medical University (No. KD2021KYJJZD009 and KD2022KYJJZD002, Kanada College of Nanjing Medical University), and the Education Research Project of Kangda College of Nanjing Medical University (KD2021JYYJYB010, Kanada College of Nanjing Medical University).

Institutional Review Board Statement: Not applicable.

Informed Consent Statement: Not applicable.

Data Availability Statement: The data presented in this study are available on request from the corresponding author. The data are not publicly available due to restrictions.

Conflicts of Interest: The authors declare no conflict of interest.

References

1. Peers, G.; Price, N.M. Copper-containing plastocyanin used for electron transport by an oceanic diatom. *Nature* **2006**, *441*, 341–344. [[CrossRef](#)] [[PubMed](#)]
2. Uauy, R.; Olivares, M.; Gonzalez, M. Essentiality of copper in humans. *Am. J. Clin. Nutr.* **1998**, *67*, 952S–959S. [[CrossRef](#)] [[PubMed](#)]
3. Linder, M.C.; Hazegh-Azam, M. Copper biochemistry and molecular biology. *Am. J. Clin. Nutr.* **1996**, *63*, 797S–811S. [[CrossRef](#)] [[PubMed](#)]
4. Gaggelli, E.; Kozłowski, H.; Valensin, D.; Valensin, G. Copper homeostasis and neurodegenerative disorders (Alzheimer's, prion, and Parkinson's diseases and amyotrophic lateral sclerosis). *Chem. Rev.* **2006**, *106*, 1995–2044. [[CrossRef](#)] [[PubMed](#)]
5. Strausak, D.; Mercer, J.F.B.; Dieter, H.H.; Stremmel, W.; Multhaup, G. Copper in disorders with neurological symptoms: Alzheimer's, Menkes, and Wilson diseases. *Brain Res. Bull.* **2001**, *55*, 175–185. [[CrossRef](#)]
6. Tsvetkov, P.; Coy, S.; Petrova, B.; Dreishpoon, M.; Verma, A.; Abdusamad, M.; Rossen, J.; Joesch-Cohen, L.; Humeidi, R.; Spangler, R.D.; et al. Copper induces cell death by targeting lipoylated TCA cycle proteins. *Science* **2022**, *375*, 1254–1261. [[CrossRef](#)]
7. Sun, J.Z.; Xu, X.; Yu, G.H.; Li, W.N.; Shi, J.S. Coumarin-based tripodal chemosensor for selective detection of Cu(II) ion and resultant complex as anion probe through a Cu(II) displacement approach. *Tetrahedron* **2018**, *74*, 987–991. [[CrossRef](#)]
8. Meng, X.J.; Cao, D.L.; Hu, Z.Y.; Han, X.H.; Li, Z.C.; Liang, D.; Ma, W.B. A coumarin based highly selective fluorescent chemosensor for sequential recognition of Cu^{2+} and PPI. *Tetrahedron Lett.* **2018**, *59*, 4299–4304. [[CrossRef](#)]
9. Amjadi, M.; Abolghasemi-Fakhri, Z. Gold nanostar-enhanced chemiluminescence probe for highly sensitive detection of Cu(II) ions. *Sens. Actuators B Chem.* **2018**, *257*, 629–634. [[CrossRef](#)]
10. Yu, Y.Y.; Yu, C.; Yin, T.X.; Ou, S.S.; Sun, X.Y.; Wen, X.R.; Zhang, L.; Tang, D.Q.; Yin, X.X. Functionalized poly (ionic liquid) as the support to construct a ratiometric electrochemical biosensor for the selective determination of copper ions in AD rats. *Biosens. Bioelectron.* **2017**, *87*, 278–284. [[CrossRef](#)]
11. Al-Nidawi, M.; Alshana, U. Reversed-phase switchable-hydrophilicity solvent liquid-liquid microextraction of copper prior to its determination by smartphone digital image colorimetry. *J. Food Compos. Anal.* **2021**, *104*, 104140. [[CrossRef](#)]
12. Gamela, R.R.; Costa, V.C.; Pereira, E.R. Multivariate Optimization of Ultrasound-Assisted Extraction Procedure for the Determination of Ca, Fe, K, Mg, Mn, P, and Zn in Pepper Samples by ICP OES. *Food Anal. Method.* **2020**, *13*, 69–77. [[CrossRef](#)]
13. Bonin, M.; Lariviere, D.; Povinec, P.P. Detection of radium at the attogram per gram level in copper by inductively coupled plasma mass spectrometry after cation-exchange chromatography. *Anal. Methods* **2020**, *12*, 2272–2278. [[CrossRef](#)]
14. Zhou, Z.L.; Tang, H.H.; Chen, S.Y.; Huang, Y.H.; Zhu, X.H.; Li, H.T.; Zhang, Y.Y.; Yao, S.Z. A turn-on red-emitting fluorescent probe for determination of copper(II) ions in food samples and living zebrafish. *Food Chem.* **2021**, *343*, 128513. [[CrossRef](#)]

15. Zhang, Y.D.; Cai, Y.H.; He, Y.H.; Lin, Q.L.; Ren, J.L.; Cao, D.S.; Zhang, L. A label-free fluorescent peptide probe for sensitive and selective determination of copper and sulfide ions in aqueous systems. *RSC Adv.* **2021**, *11*, 7426–7435. [[CrossRef](#)]
16. Zeng, X.D.; Gao, S.; Jiang, C.; Duan, Q.X.; Ma, M.S.; Liu, Z.G.; Chen, J. Rhodol-derived turn-on fluorescent probe for copper ions with high selectivity and sensitivity. *Luminescence* **2021**, *36*, 1761–1766. [[CrossRef](#)]
17. Liu, J.Q.; Liu, Z.C.; Wang, W.K.; Tian, Y. Real-time Tracking and Sensing of Cu⁺ and Cu²⁺ with a Single SERS Probe in the Live Brain: Toward Understanding Why Copper Ions Were Increased upon Ischemia. *Angew. Chem. Int. Ed.* **2021**, *60*, 21351–21359. [[CrossRef](#)]
18. Sun, X.Y.; Liu, T.; Sun, J.; Wang, X.J. Synthesis and application of coumarin fluorescence probes. *RSC Adv.* **2020**, *10*, 10826–10847. [[CrossRef](#)]
19. Wang, K.N.; Sun, P.Z.; Chao, X.J.; Cao, D.X.; Mao, Z.W.; Liu, Z.Q. A coumarin Schiff's base two-photon fluorescent probe for hypochlorite in living cells and zebrafish. *RSC Adv.* **2018**, *8*, 6904–6909. [[CrossRef](#)]
20. He, G.J.; Hua, X.B.; Yang, N.; Li, L.L.; Xu, J.H.; Yang, L.L.; Wang, Q.Z.; Ji, L.G. Synthesis and application of a "turn on" fluorescent probe for glutathione based on a copper complex of coumarin hydrazide Schiff base derivative. *Bioorg. Chem.* **2019**, *91*, 103176. [[CrossRef](#)]
21. Yan, L.Q.; Hu, C.J.; Li, J.P. A fluorescence turn-on probe for rapid monitoring of hypochlorite based on coumarin Schiff base. *Anal. Bioanal. Chem.* **2018**, *410*, 7457–7464. [[CrossRef](#)]
22. Wang, Y.; Hao, X.H.; Liang, L.X.; Gao, L.Y.; Ren, X.M.; Wu, Y.G.; Zhao, H.C. A coumarin-containing Schiff base fluorescent probe with AIE effect for the copper(II) ion. *RSC Adv.* **2020**, *10*, 6109–6113. [[CrossRef](#)]
23. Mani, K.S.; Rajamanikandan, R.; Ravikumar, G.; Pandiyan, B.V.; Kolandaivel, P.; Ilanchelian, M.; Rajendran, S.P. Highly Sensitive Coumarin-Pyrazolone Probe for the Detection of Cr³⁺ and the Application in Living Cells. *ACS Omega* **2018**, *3*, 17212–17219. [[CrossRef](#)]
24. Babur, B.; Seferoglu, N.; Seferoglu, Z. A coumarin-pyrazolone based fluorescent probe for selective colorimetric and fluorimetric fluoride detection: Synthesis, spectroscopic properties and DFT calculations. *J. Mol. Struct.* **2018**, *1161*, 218–225. [[CrossRef](#)]
25. Babur, B.; Seferoglu, N.; Ocal, M.; Sonugur, G.; Akbulut, H.; Seferoglu, Z. A novel fluorescence turn-on coumarin-pyrazolone based monomethine probe for biothiol detection. *Tetrahedron* **2016**, *72*, 4498–4502. [[CrossRef](#)]
26. Honglei, L.; Pengyu, C.; Juan, L.; Sai, C.; Meng, W. Coumarin Pyrazolone Fluorescent Probe as Well as Preparation Method and Application Thereof. CN202210882392.3[P]. 11 November 2022. Available online: <https://d.wanfangdata.com.cn/patent/CN202210882392.3> (accessed on 1 November 2023).
27. Vijay, K.; Nandi, C.; Samant, S.D. Synthesis of a dihydroquinoline based merocyanine as a 'naked eye' and 'fluorogenic' sensor for hydrazine hydrate in aqueous medium and hydrazine gas. *RSC Adv.* **2014**, *4*, 30712–30717. [[CrossRef](#)]
28. Surati, K.R.; Thaker, B.T. Synthesis, spectroscopic and thermal investigation of Schiff-base complexes of Cu(II) derived from heterocyclic beta-diketone with various primary amines. *J. Coord. Chem.* **2006**, *59*, 1191–1202. [[CrossRef](#)]
29. Naik, M.D.; Bodke, Y.D.; Kumar, V.M.; Revanasiddappa, B.C. An efficient one-pot synthesis of coumarin-amino acid derivatives as potential anti-inflammatory and antioxidant agents. *Synth. Commun.* **2020**, *50*, 1210–1216. [[CrossRef](#)]
30. Taha, M.; Shah, S.A.A.; Afifi, M.; Imran, S.; Sultan, S.; Rahim, F.; Khan, K.M. Synthesis, alpha-glucosidase inhibition and molecular docking study of coumarin based derivatives. *Bioorg. Chem.* **2018**, *77*, 586–592. [[CrossRef](#)]
31. Xia, X.C.; Fu, Y.; Tang, H.; Li, Y.; Wang, F.Y.; Ren, J. A self-assembled micellar nanoprobe for specific recognition of hydrazine in vitro and in vivo. *Sens. Actuators B Chem.* **2018**, *272*, 479–484. [[CrossRef](#)]
32. Yin, J.; Wang, Z.; Zhao, F.; Yang, H.; Li, M.; Yang, Y. A novel dual functional pyrene-based turn-on fluorescent probe for hypochlorite and copper (II) ion detection and bioimaging applications. *Spectrochim. Acta Part A Mol. Biomol. Spectrosc.* **2020**, *239*, 118470. [[CrossRef](#)] [[PubMed](#)]
33. Wang, Y.Y.; Ai, Y.; Zhang, Y.L.; Ren, Y.Y.; Wang, J.L.; Yao, F.Y.; Li, W.Y.; Zhou, Y.; Sun, Y.N.; Liu, J.L.; et al. A new probe with high selectivity and sensitivity for detecting copper ions in traditional Chinese medicine and water sample. *Inorg. Chem. Commun.* **2021**, *128*, 108563. [[CrossRef](#)]
34. Wang, M.M.; Wang, C.; Wang, M.; Sun, T.M.; Huang, Y.; Tang, Y.F.; Ju, J.F.; Shen, L.J.; Hu, Y.Y.; Zhu, J.L. A Dual-Functional "On-Off-On" Relay Fluorescent Probe for the Highly Sensitive Detection of Copper(II) and Phosphate Ions. *ChemistrySelect* **2020**, *5*, 1331–1334. [[CrossRef](#)]
35. Anand, T.; Sivaraman, G.; Chellappa, D. Quinazoline copper(II) ensemble as turn-on fluorescence sensor for cysteine and chemodosimeter for NO. *J. Photochem. Photobiol. A* **2014**, *281*, 47–52. [[CrossRef](#)]
36. Arslan, F.N.; Geyik, G.A.; Koran, K.; Ozen, F.; Aydin, D.; Elmas, S.N.K.; Gorgulu, A.O.; Yilmaz, I. Fluorescence "Turn On-Off" Sensing of Copper (II) Ions Utilizing Coumarin-Based Chemosensor: Experimental Study, Theoretical Calculation, Mineral and Drinking Water Analysis. *J. Fluoresc.* **2020**, *30*, 317–327. [[CrossRef](#)] [[PubMed](#)]
37. Kim, G.; Choi, D.; Kim, C. A Benzothiazole-Based Fluorescence Turn-on Sensor for Copper(II). *J. Fluoresc.* **2021**, *31*, 1203–1209. [[CrossRef](#)] [[PubMed](#)]
38. Silpcharu, K.; Soonthonhut, S.; Sukwattanasinitt, M.; Rashatasakhon, P. Fluorescent Sensor for Copper(II) and Cyanide Ions via the Complexation-Decomplexation Mechanism with Di(bissulfonamido)spirobifluorene. *ACS Omega* **2021**, *6*, 16696–16703. [[CrossRef](#)]

39. Tamil Selvan, G.; Varadaraju, C.; Tamil Selvan, R.; Enoch, I.; Mosae Selvakumar, P. On/Off Fluorescent Chemosensor for Selective Detection of Divalent Iron and Copper Ions: Molecular Logic Operation and Protein Binding. *ACS Omega* **2018**, *3*, 7985–7992. [[CrossRef](#)]
40. Rupa, S.A.; Patwary, M.A.M.; Ghann, W.E.; Abdullahi, A.; Uddin, A.K.M.R.; Mahmud, M.M.; Haque, M.A.; Uddin, J.; Kazi, M. Synthesis of a novel hydrazone-based compound applied as a fluorescence turn-on chemosensor for iron(iii) and a colorimetric sensor for copper(ii) with antimicrobial, DFT and molecular docking studies. *RSC Adv.* **2023**, *13*, 23819–23828. [[CrossRef](#)]
41. Zhang, Y.P.; Teng, Q.; Yang, Y.S.; Guo, H.C.; Xue, J.J. A novel coumarin-based pyrazoline fluorescent probe for detection of Fe³⁺ and its application in cells. *Inorg. Chim. Acta* **2021**, *525*, 120469. [[CrossRef](#)]
42. Zong, L.Y.; Wang, C.; Song, Y.C.; Hu, J.; Li, Q.Q.; Li, Z. A fluorescent and colorimetric probe based on naphthalene diimide and its high sensitivity towards copper ions when used as test strips. *RSC Adv.* **2019**, *9*, 12675–12680. [[CrossRef](#)] [[PubMed](#)]

Disclaimer/Publisher's Note: The statements, opinions and data contained in all publications are solely those of the individual author(s) and contributor(s) and not of MDPI and/or the editor(s). MDPI and/or the editor(s) disclaim responsibility for any injury to people or property resulting from any ideas, methods, instructions or products referred to in the content.